Geospatial Assessment of Soil Salinity in an Urban Coastal Environment: A Case Study of Chennai Metropolitan Region, Southern India

Sundaramoorthy Sridhar[1,2*], Moorthy Prabhakaran[1], Abdul Rahim Ahamed Ibrahim[1] and Chokkalingam Lakshumanan[1]

1. Centre for Disaster Management and Coastal Research, Department of Remote Sensing, Bharathidasan University, Tiruchirappalli, Tamil Nadu, INDIA
2. Water Resources Department, Chennai, Tamil Nadu, INDIA
*sridharddg1971@gmail.com

Abstract

Soil salinization is a growing environmental issue in coastal urban regions, impacting land productivity, vegetation health and infrastructure. This study provides a geospatial assessment of soil salinity across the Chennai Metropolitan Region using multi-temporal Landsat 8 OLI imagery and spectral salinity indices. Thirteen indices including SI, SI1–SI4, SR, RSI, MSR, NDSI, NDVI, GNDVI, SAVI, DVI, VSSI and EVI were used to capture surface reflectance and vegetation degradation. An integrated machine learning-based overlay analysis using Random Forest (RF) classified salinity into five categories: very low, low, moderate, high and very high. Results indicate that the northern coastal belt of Chennai, especially areas near the Bay of Bengal, falls under high to very high salinity due to tidal intrusion, urbanization and inadequate drainage. Inland zones like Madhavaram, Ambattur, Alandur, Guindy, Velachery and Sholinganallur showed low to moderate salinity levels. Landuse Land Cover (LULC) data for 2025 was incorporated to examine spatial correlations between salinity and urban expansion.

This study highlights the effectiveness of combining spectral indices with machine learning to identify salinity hotspots and support informed urban planning and sustainable land management in vulnerable coastal megacities.

Keywords: Soil salinity, Remote sensing, Spectral indices, Machine learning, Random Forest and Urban planning.

Introduction

Soil salinity is a critical form of land degradation that adversely affects agricultural productivity, ecological health and infrastructure stability, especially in coastal regions where seawater intrusion and urban expansion intersect[8,29]. Excessive accumulation of soluble salts in the soil profile leads to a decline in soil fertility, reduced plant growth and increased surface crusting, all of which have significant implications for food security and sustainable land use[3,27]. In urbanizing coastal environments like Chennai, salinity is further exacerbated by unplanned development, rising sea levels, groundwater over-extraction and poor surface drainage systems[25,30]. Remote Sensing (RS) and Geographic Information Systems (GIS) have emerged as indispensable tools for mapping, monitoring and managing soil salinity at various spatial and temporal scales[1,24]. These technologies enable efficient extraction of land surface characteristics such as soil reflectance, vegetation health and topographic variations[16,26]. Spectral indices derived from satellite data - particularly those based on Landsat 8 OLI bands, offer a non-invasive means of detecting saline soils and assessing their impact on vegetation cover[14]. When integrated with machine learning (ML) algorithms, such as Random Forest (RF), the classification and prediction of salinity levels can be significantly enhanced[6].

The Chennai Metropolitan Region (CMR) faces multiple environmental challenges including coastal erosion, seawater intrusion, surface water contamination and vegetation stress[18,21]. The city's proximity to the Bay of Bengal, combined with its flat topography and increasing urban sprawl, has led to notable changes in landuse and land cover (LULC), contributing to localized salinity build up[15,28]. Regions in the northern coastal belt show high vulnerability due to direct tidal influence whereas inland zones exhibit comparatively lower levels of salinization[13]. This environmental variability necessitates a detailed and spatially explicit analysis to support mitigation and planning strategies[19].

This study aims to conduct a comprehensive geospatial assessment of soil salinity in Chennai using a multi-index approach derived from satellite-based spectral reflectance data[5,22]. Thirteen salinity and vegetation indices, including SI, SI1–SI4, NDSI, NDVI, SAVI, VSSI and EVI, are utilized to derive surface conditions. RF classifier is employed to categorize salinity levels across the study area[10]. Furthermore, LULC 2025 is used to understand the spatial relationship between land transformation and salinity severity[17]. The novelty of this research lies in its integration of multiple spectral indices with a machine learning-based classification model to produce a detailed, high-resolution salinity map for an urban coastal environment[4,12].

Unlike conventional field-based assessments, this approach provides a cost-effective, scalable and replicable method to monitor soil salinity in real time[1,11]. Additionally, by correlating salinity hotspots with urban development zones, the study contributes valuable insights for sustainable land management, climate adaptation and urban planning in rapidly growing coastal cities like Chennai[9,23].

Material and Methods

The study is focused on Chennai, the capital of Tamil Nadu, located on the south-eastern coast of India along the Bay of Bengal. The study area extends approximately 435.77 square kilometres between 12°32′N to 13°12′N latitude and 80°04′E to 80°20′E longitude (Figure 1). Chennai is a major metropolitan hub with a population exceeding 10 million, making it one of the largest and most densely populated cities in India. The city experiences a tropical wet and dry climate, with peak rainfall during the northeast monsoon. The region's flat terrain and low elevation, combined with coastal location, make it highly susceptible to flooding, saline water intrusion and land degradation, especially in low-lying and peri-urban regions.

Urban expansion, coupled with reclamation of wetlands, unregulated construction and groundwater over-extraction, has intensified the environmental stress on the region. Soil salinization has become a pressing issue, particularly in the northern and southeastern parts of Chennai, where increased surface reflectance and vegetation loss are evident. These changes have adversely impacted agricultural viability, ecological stability and infrastructure longevity. To address these challenges, it is essential to implement a spatially informed monitoring framework that integrates remote sensing indices to detect and analyse soil salinity and vegetation stress. Such analysis provides crucial insights for urban planners, environmental managers and policymakers to identify vulnerable zones, guide sustainable development and mitigate long-term risks associated with land degradation and environmental change in Chennai.

The region is characterized by coastal climatic conditions, making it susceptible to soil salinization, urban expansion and vegetation stress[24]. Satellite imagery for April 2025 was acquired from the United States Geological Survey (USGS) Earth Explorer portal using Landsat 8 OLI/TIRS data[27]. April was chosen to represent pre-monsoon dry conditions, when salinity effects are more pronounced and vegetation stress becomes spatially evident.

The satellite data underwent radiometric and atmospheric correction. Band combinations were used to derive various spectral indices using the raster calculator in ArcGIS[16]. Each index is used to detect soil salinity, vegetation health, or both[15].

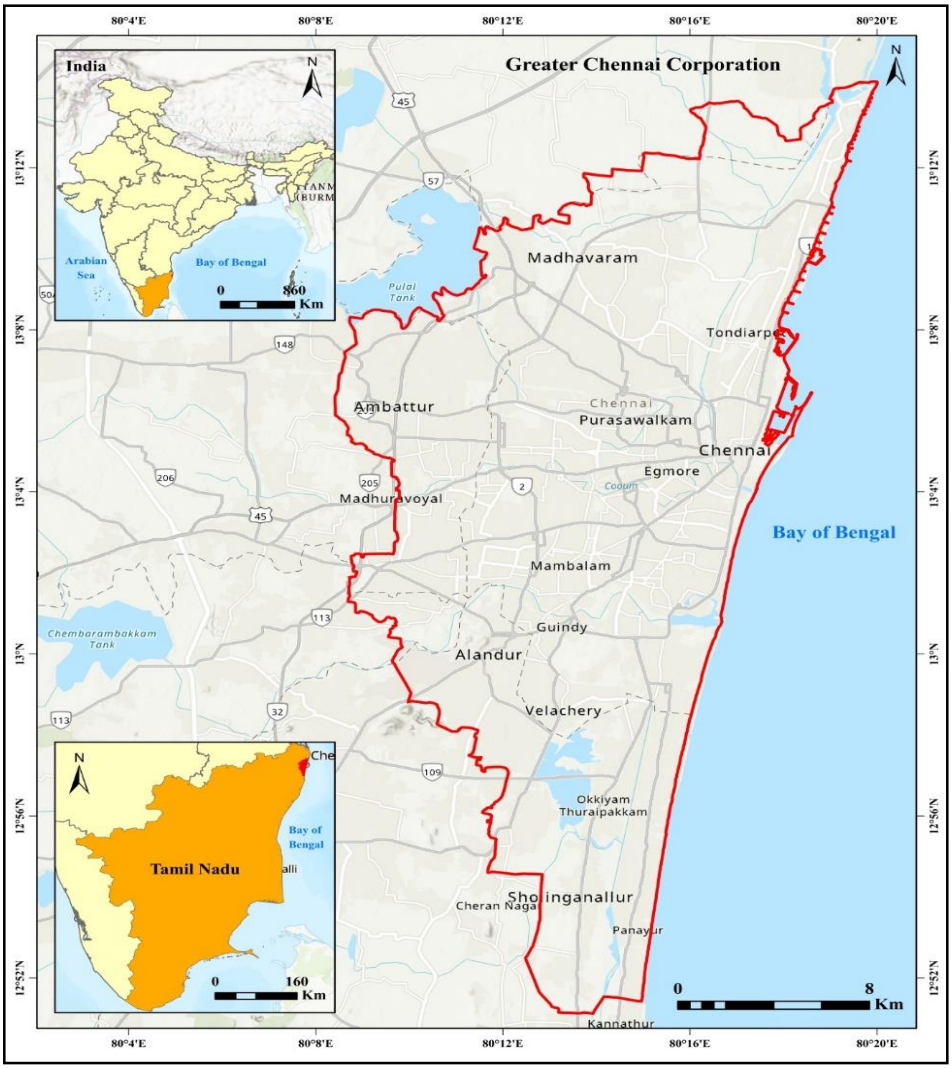

Figure 1: Study area location map

Table 1
Spectral Indices and Formulas Used for Salinity and Vegetation Assessment

S.N.	Index	Formula
1.	Salinity Index (SI)[8,11]	$SI = \sqrt{Blue * Red}$
2.	Salinity Index 1 (SI1)[14]	$SI1 = \frac{Blue}{Red}$
3.	Salinity Index 2 (SI2)[17]	$SI2 = \frac{(Blue-Red)}{(Blue+Red)}$
4.	Salinity Index 3 (SI3)[20]	$SI3 = \frac{(Green*Red)}{Blue}$
5.	Salinity Index 4 (SI4)[21]	$SI4 = \frac{(NIR*Red)}{Green}$
6.	Simple Ratio (SR)[19]	$SR = \frac{(Red-NIR)}{(Green+NIR)}$
7.	Ratio Spectral Index (RSI)[22]	$RSI = \frac{Red}{NIR}$
8.	Mosaic Simple Ratio (MSR)[26]	$MSR = \frac{NIR}{Red}$
9.	Normalized Difference Salinity Index (NDSI)[28]	$NDSI = \frac{(Red-NIR)}{(Red+NIR)}$
10.	Normalized Difference Vegetation Index (NDVI)[2]	$NDVI = \frac{(NIR-Red)}{(NIR+Red)}$
11.	Green Normalized Difference Vegetation Index (GNDVI)[1]	$GNDVI = \frac{(NIR-Green)}{(NIR+Green)}$
12.	Soil Adjusted Vegetation Index (SAVI)[4]	$SAVI = \frac{(NIR - Red)}{(NIR + Red) + L\ *(1-L)}$
13.	Differential Vegetation Index (DVI)[7]	$DVI = NIR - Red$
14.	Vegetation Soil Salinity Index (VSSI)[12]	*VSSI = 2 * Green – 5 * (Red + NIR) * Green – 5 * (Red + NIR)*
15.	Enhanced Vegetation Index (EVI)[29]	$EVI = 2.5 * \frac{NIR-RED}{NIR+(6*RED-7.5*Blue)+1}$
16.	Brightness Index (BI)[30]	$BI = \sqrt{\frac{Red^2+Green^2}{2}}$

Salinity indices are spectral indicators derived from remote sensing data that help to detect and monitor salt-affected soils based on their unique reflectance characteristics in different wavelength bands[10]. Soil salinity alters the surface reflectance, typically increasing brightness in the visible (Blue, Green, Red) bands and decreasing reflectance in the near-infrared (NIR) band due to reduced vegetation cover and soil crusting (Table 1)[13].

Machine Learning Technique

Model Selection and Implementation: Extreme gradient boosting (XGBoost) algorithm was employed due to its superior performance in classification and regression tasks, handling of non-linearity and resistance to over fitting through regularization. The model was trained using spectral indices derived from satellite data as input features. These include salinity indices, vegetation indices and brightness indices known to correlate with soil salinity. The training dataset was split into training (70%) and testing (30%) subsets. Feature standardization was applied before model training.

The XGBoost model is based on gradient boosting decision trees, where a series of weak learners (trees) are combined to create a strong learner. The objective function of XGBoost is defined as:

$$L(\emptyset) = \sum_{i=1}^{n} l\left(yi, \hat{Y}i\right) + \sum_{k=1}^{K} \Omega(\text{fk}) \quad (1)$$

where $l\left(yi, \hat{Y}i\right)$ is loss function that measures the difference between the prediction $\hat{Y}i$ and the actual target yi, $\Omega(\text{fk})$ is $\gamma T + \frac{1}{2}\lambda \sum_{j=1}^{T} w_j^2$ for regularization of term controlling model complexity, T is number of leaves in the tree, wj is weight of the j[th] leaf and γ, λ is regularization parameters.

The prediction of an instance is obtained by summing the outputs of all regression trees:

$$\hat{Y} = \sum_{k=1}^{K} f_k(x_i), \quad f_k \epsilon f \quad (2)$$

where f is space of regression trees, f_k is individual tree function. Model tuning was carried out using grid search and cross-validation for parameters including learning rate (η), maximum depth, subsample ratio, column sample by tree and number of boosting rounds.

Table 2
Accuracy Metrics and Formulae for Salinity Classification Model Evaluation

Metrics	Formulae	Description
Overall Accuracy (OA)	$OA = \frac{\sum_{i=1}^{n} C_{ii}}{N}$	C_{ii} is the correctly classified samples for class i and N is the total number of samples.
Kappa Coefficient (κ):	$k = \frac{p_o - p_e}{1 - p_e}$	p_o is observed agreement and p_e is expected agreement by chance.
Precision (P):	$P = \frac{TP}{TP+FP}$	TP is True Positives, FP: False Positives, FN: False Negatives. The XGBoost model was implemented in Python using the XGBoost library. The final trained model was used to generate salinity zone maps over the study area, which were validated against ground truth and existing salinity data.
Recall (R):	$R = \frac{TP}{TP+FN}$	
F1 Score:	$F1 = 2 * \frac{P*R}{P+R}$	

Accuracy Assessment: To evaluate the performance of the XGBoost model in salinity classification, the following accuracy metrics were computed using the confusion matrix derived from predicted vs. actual salinity zones (Table 2).

Landuse and Land Cover Mapping: Landsat 8 OLI and Landsat 9 imagery (30 m resolution) from April 2025 were used for Land Use and Land Cover (LULC) mapping. Cloud-free images were pre-processed through radiometric calibration, atmospheric correction (DOS1) and mosaicking. The NRSC Level-3 classification scheme guided interpretation using false colour composites (FCC) from bands 5, 4 and 3. Visual interpretation was performed onscreen in ArcGIS at a 1:10,000 scale using keys like tone, texture, shape and association. Ancillary data, including topographic maps, prior LULC maps and Google Earth imagery, supported accurate feature delineation. The final LULC map was overlaid with a soil salinity classification map generated using the XGBoost model.

This integrated analysis revealed that salinity predominantly affected fallow lands, sandy areas, swampy lands and land without scrub. The study highlights the spatial correlation between LULC patterns and soil salinity, offering valuable inputs for targeted land management and reclamation strategies.

Results and Discussion

The application of the XGBoost machine learning model for soil salinity mapping utilized a suite of spectral indices derived from satellite imagery[21]. These indices were selected for their relevance in detecting surface reflectance changes influenced by salinity and vegetation stress[26]. The spatial variation and statistical range of each index are presented in figure 2 to 5. Figure 2 highlights the spatial distribution of salinity-specific indices. The salinity index (SI) (Figure 2a) ranges from –0.45 to 0.63, exhibiting moderate spatial variability across the region. Elevated SI values are observed in coastal and low-lying inland zones, indicating areas prone to salt accumulation[27]. Salinity index 1 (SI1) (Figure 2b), with a range from –0.23 to 0.72, demonstrates higher sensitivity in detecting saline patches, particularly over sparsely vegetated and bare soil regions[30]. Salinity index 2 (SI2) (Figure 2c) spans from –0.61 to 0.11 and shows predominantly negative values, possibly due to surface moisture or organic matter suppressing salinity signals[24]. Meanwhile, salinity index 3 (SI3) (Figure 2d) ranges from –0.49 to 0.18, highlighting regions with reduced salinity expression, often influenced by clayey or shaded areas[22]. Figure 3 presents ratio-based indices that further refine salinity detection. Salinity index 4 (SI4) (Figure 3a) ranges from –0.08 to 0.42, balancing responses from soil brightness and vegetative stress[23]. Simple ratio (SR) (Figure 3b), with values from –0.47 to 0.37, shows negative values in regions dominated by non-photosynthetic or salt-affected surfaces[19].

Ratio spectral index (RSI) (Figure 3c) ranges from –0.76 to 0.35, offering enhanced sensitivity to surface reflectance where salt crusting is prevalent[29]. The Mosaic simple ratio (MSR) (Figure 3d), ranging from –0.32 to 0.79, captures strong spectral contrasts in heterogeneous land-use zones, particularly in agricultural-fallow transitions often associated with salinity accumulation[14].

Figure 4 features normalized indices that integrate vegetation responses as proxies for salinity stress. The Normalized Difference Salinity Index (NDSI) (Figure 4a) ranges from –0.49 to 0.13 where negative values dominate, highlighting vegetative degradation due to salinity[5]. The Normalized Difference Vegetation Index (NDVI) (Figure 4b), with a range from –0.13 to 0.49, reveals clear distinctions in vegetation vigor, with NDVI values below 0.2 aligning with moderate to high salinity zones[7]. The Green Normalized Difference Vegetation Index (GNDVI) (Figure 4c), spanning –0.14 to 0.44, displays increased sensitivity to chlorophyll variations, especially in semi-arid or salt-stressed zones[12].

Soil Adjusted Vegetation Index (SAVI) (Figure 4d) ranges from –0.11 to 0.74 and performs effectively in areas with partial vegetation cover by minimizing soil background effects[18]. Figure 5 illustrates additional indices that capture vegetation degradation and soil reflectance properties. The Differential Vegetation Index (DVI) (Figure 5a), ranging from –0.02 to 0.17, shows limited contrast but is useful for detecting subtle vegetation variations linked to salt stress[15].

The Vegetation Soil Salinity Index (VSSI) (Figure 5b), with values from –0.07 to 0.73, offers a comprehensive view of both vegetation health and soil salinity, with higher values marking saline-affected zones[13].

The Enhanced Vegetation Index (EVI) (Figure 5c), varying between –0.09 and 0.72, is especially effective in capturing vegetation stress responses in moderately saline environments[10]. Lastly, the Brightness Index (BI) (Figure 5d) spans from –0.74 to 0.25, highlighting areas with high surface reflectance commonly associated with salt-encrusted or bare soils[8]. These indices collectively serve as robust indicators of salinity zones and are critical inputs for the XGBoost model[1].

The variation in their spatial ranges and distributions underscores the complex interplay between soil salinity, vegetation stress and surface reflectance, providing a solid foundation for the machine learning-based classification framework[4]. Figure 6 illustrates the soil salinity zones map for Chennai, Tamil Nadu, India. Figure 8 illustrates profile graph for validation of soil salinity zones using XGBoost model for Chennai, Tamil Nadu, India. In the north coast of Chennai, other regions such as Ennore, Mylapore, Velachery and Egmore exhibit high to very high soil salinity**,** primarily due to their proximity to the coast, tidal influence, poor drainage conditions and potential seawater intrusion into the shallow aquifers[6]. These areas also experience anthropogenic stress from industrial activity and urban runoff, which can exacerbate salinity accumulation in surface and sub-surface soils.

In contrast, localities like Saidapet, Anna Nagar, Kolathur and Medavakkam fall within low to very low salinity zones, likely owing to better drainage, relatively higher elevation and less direct exposure to coastal influence[1]. These areas benefit from more stable land use including vegetated cover or infrastructure that reduces soil salinization, indicating spatial variability in salinity distribution closely linked to geomorphology, hydrology and urban development intensity[6].

Figure 9 illustrates the estimated area distribution of soil salinity zones in the study area. The bar graph shows that very high salinity zones occupy the largest area at 145.86 sq.km, indicating severe salt accumulation. This is followed by very low salinity zones with 89.65 sq.km, suggesting relatively healthy soil conditions. High salinity zones cover 75.46 sq.km, while low and moderate salinity zones span 65.36 sq.km and 59.78 sq.km respectively. The north coast of Chennai is characterized by high to very high soil salinity levels, particularly in zones directly influenced by coastal proximity, estuarine activity and industrial discharg[8]. This region is geographically low-lying and is subjected to frequent tidal influx, poor natural drainage and seawater intrusion, especially during dry seasons or groundwater over-extraction[10].

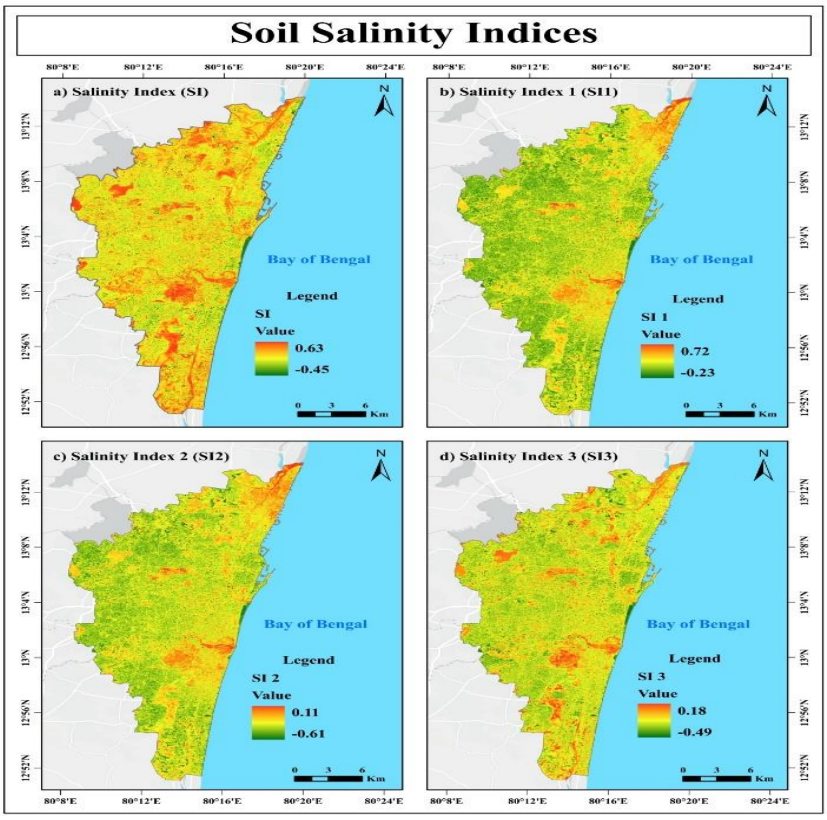

Figure 2: a) Salinity Index (SI), b) Salinity Index 1 (SI1), c) Salinity Index 2 (SI2) and d) Salinity Index 3 (SI3) for Chennai, Tamil Nadu, India

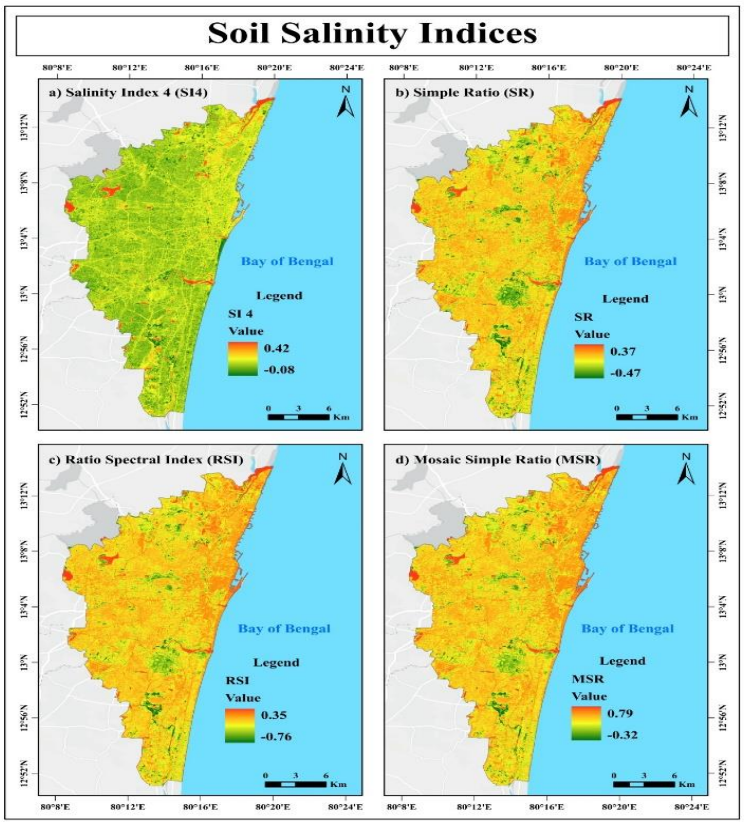

Figure 3: a) Salinity Index 4 (SI4), b) Simple Raito (SR), c) Ratio Spectral Index (RSI) and d) Mosaic Simple Ratio (MSR) for Chennai, Tamil Nadu, India

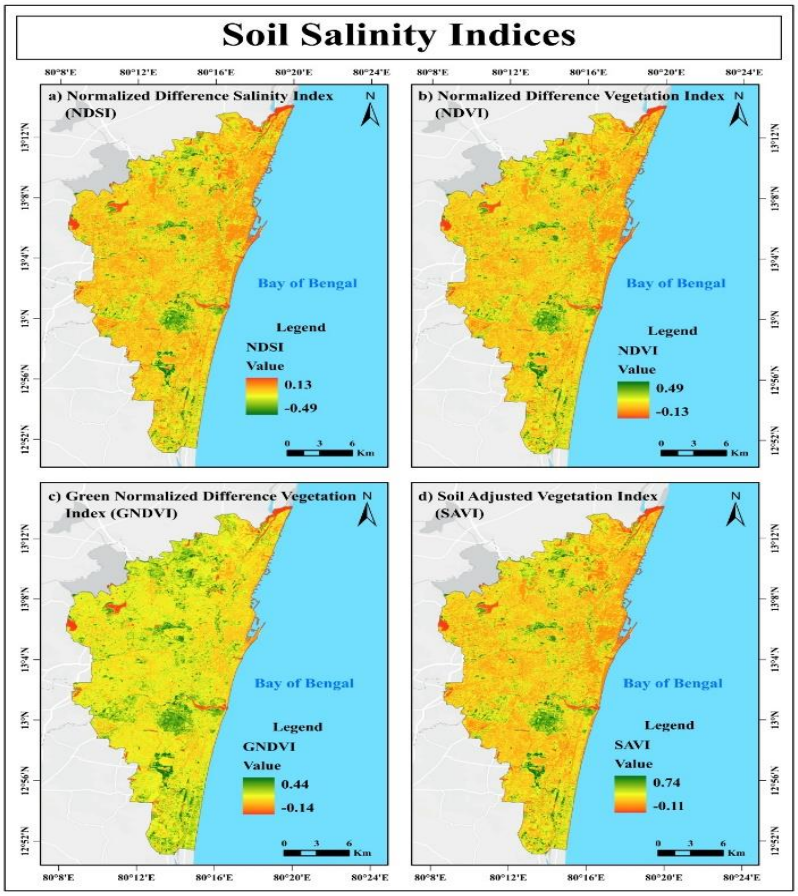

Figure 4: a) NDSI, b) NDVI, c) GNDVI and d) SAVI for Chennai, Tamil Nadu, India

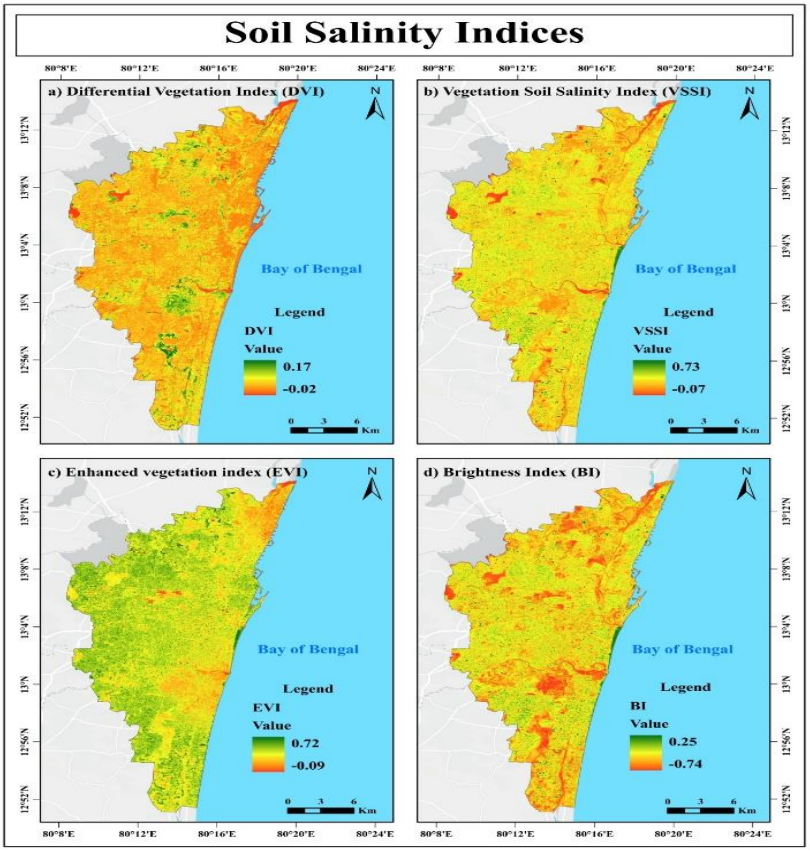

Figure 5: a) DVI, b) VSSI, c) EVI and d) Brightness Index (BI) for Chennai, Tamil Nadu, India

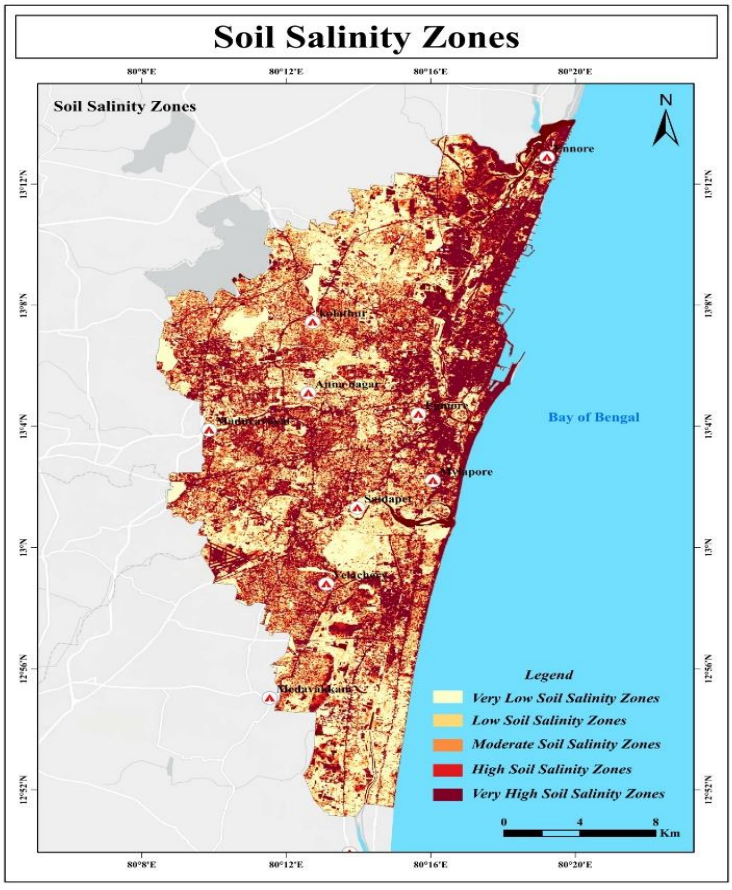

Figure 6: Soil Salinity Zones Map using XGBoost Model for Chennai, Tamil Nadu, India

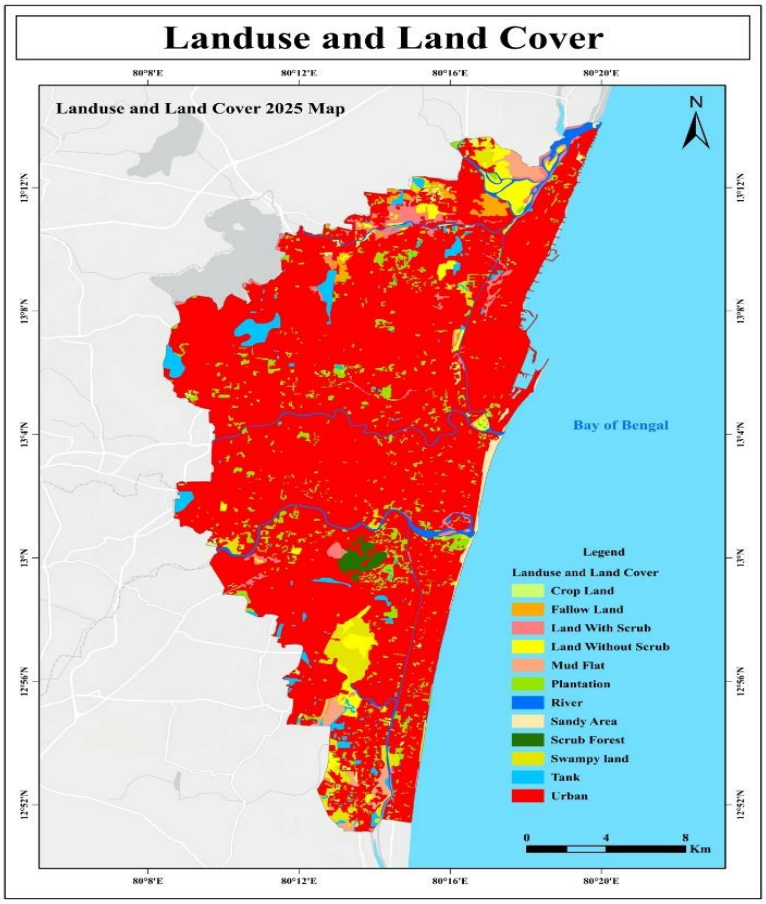

Figure 7: Landuse and land cover Map (2025) for Chennai, Tamil Nadu, India

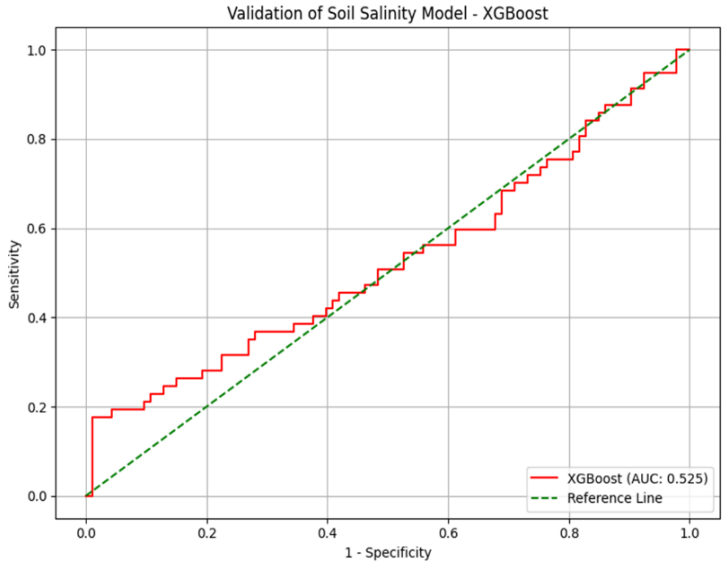

Figure 8: Profile graph for validation of soil salinity zones using XGBoost model for Chennai, Tamil Nadu, India

The presence of salt pans, marshy wetlands and heavy urban-industrial pressure further accelerates the accumulation of surface salts[12]. As a result, soils in the northern coastal stretch of Chennai tend to exhibit elevated salinity, making them less suitable for agriculture and more prone to ecological degradation, requiring careful monitoring and management for sustainable land use and environmental health[13].

Landuse and land Cover 2025: The visual interpretation of Landsat 8/9 imagery for April 2025, following the NRSC Level-3 classification system, enabled the detailed mapping of landuse and land cover (LULC) categories across the study area in figure 7. The results are summarized in terms of spatial extent (in square kilometres), as shown in figure 10 and percentage as shown in figure 11. The urban category is the most dominant landuse type, occupying approximately

345.98 km² (79.3%), which indicates extensive urbanization and built-up development in the region. This suggests potential impervious surface expansion and anthropogenic pressure on surrounding natural and agricultural zones[14]. Plantation areas constitute the second largest class, covering 21.96 km² (5%). These are primarily located in the peri-urban and agricultural fringe zones and include managed tree crops or agroforestry practices[7].

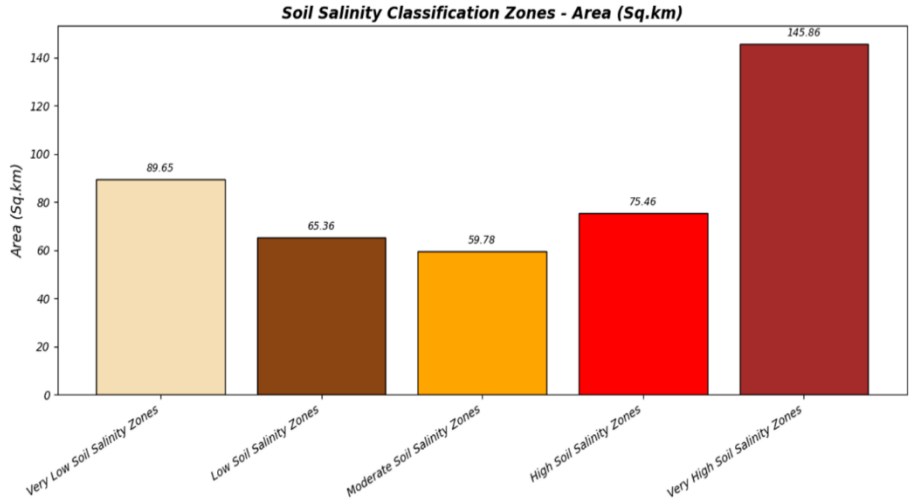

Figure 9: Soil Salinity Classification Zones area (sq.km) estimation for Chennai, Tamil Nadu, India

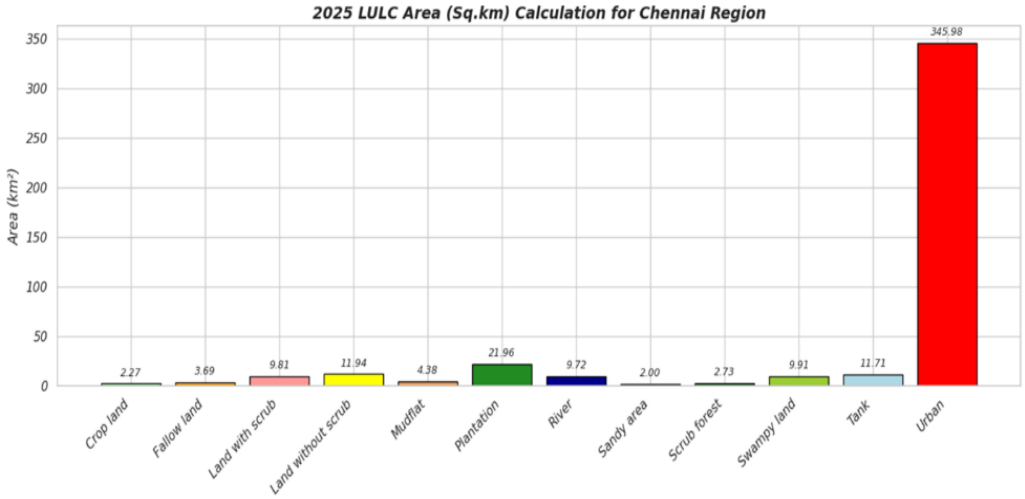

Figure 10: LULC Classification area (sq.km) estimation for Chennai, Tamil Nadu, India

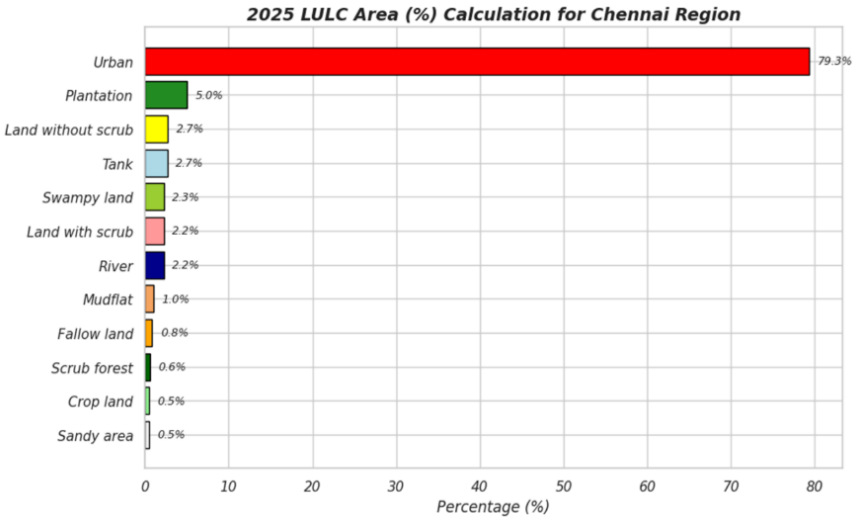

Figure 11: LULC Classification area (%) estimation for Chennai, Tamil Nadu, India

Land without scrub and land with scrub account for 11.94 km² (2.7%) and 9.81 km² (2.2%) respectively[4]. These categories represent degraded or semi-natural landscapes, often vulnerable to erosion, salinity intrusion and seasonal vegetation stress. Tank and rivers cover 11.70 km² (2.7%) and 9.72 km² (2.2%) respectively, playing a vital role in irrigation and local hydrology[15]. However, proximity of tanks to saline-prone zones highlights the importance of monitoring water quality and seasonal recharge[21]. Swampy lands, which span 9.90 km² (2.3%), are ecologically sensitive areas prone to seasonal inundation and often coincide with moderate salinity zones, reflecting a dynamic interface between soil saturation and salt accumulation[22].

Mudflats cover 4.38 km² (1%), typically occurring along the coastal or estuarine edges and are indicative of high evaporation potential and salt crust formation[26]. Scrub forests and sandy areas account for 2.73 km² (0.6%) and 2.00 km² (0.5%) respectively. While scrub forests may support low-density vegetation under arid conditions, sandy areas have poor water retention and are often susceptible to salinization[27]. Fallow lands and croplands are relatively limited, with areas of 3.69 km² (0.8%) and 2.27 km² (0.5%) respectively. The limited presence of active cropland suggests potential constraints on agriculture, possibly due to soil degradation, salinity stress, or water scarcity[30].

When overlaid with the soil salinity classification map, it was observed that fallow lands, land with scrub, swampy areas and mudflats are significantly correlated with moderate to high salinity zones[24]. Conversely, plantation zones and active croplands are generally located in areas with lower salinity levels, highlighting the influence of soil health on land utilization patterns[19]. This spatial relationship reinforces the need for integrated land management practices to mitigate the impacts of salinity and ensure sustainable land use planning[23].

The spatial patterns of soil salinity derived using the XGBoost model and spectral indices reveal strong correlations with land cover types and proximity to the coastal environment, particularly along the north coast of Chennai. These findings are consistent with previous studies that emphasize the critical role of geomorphological and hydrological factors in salinity distribution. The coastal and low-lying urban zones are more vulnerable to saltwater intrusion and soil degradation due to sea-level rise and human disturbances[24]. The effectiveness of remote sensing-based indices in capturing subtle spectral variations associated with salinity confirmed that indices such as SI, NDVI and BI, can serve as reliable indicators for identifying salinity hotspots when combined with machine learning models like XGBoost[26,27].

The classification results also revealed that areas with vegetative stress and exposed soils, such as fallow lands, scrublands and mudflats, showed stronger salinity signals while plantation and cropland regions typically coincided with zones of lower salinity. These observations support that vegetation indices (EVI, SAVI) are negatively correlated with salinity and can be used to infer soil condition indirectly[29,30]. The high salinity observed along Chennai's northern coastal belt is also in agreement with studies, which emphasize the need for localized soil and water conservation strategies in urbanizing coastal regions[21,22]. The study also benefited from accurate reflectance correction and data preprocessing methods ensuring the reliability of Landsat-based salinity mapping[19]. Furthermore, the overlay of LULC with salinity zones provides valuable insights for urban planning and agricultural sustainability. Urban expansion over saline-prone zones can exacerbate land degradation and environmental stress in coastal megacities[23]. This integrated geospatial approach underscores the utility of combining machine learning, spectral analysis and land cover assessment to support evidence-based land management decisions in rapidly developing coastal landscapes.

Conclusion

This study demonstrated an integrated approach for mapping and analyzing soil salinity in the north coastal region of Chennai using Landsat 8/9 satellite data, spectral indices and the XGBoost machine learning model. A comprehensive suite of salinity, vegetation and brightness indices including SI, NDSI, NDVI, SAVI, BI and VSSI was used to capture spectral variations linked to soil salinity. The XGBoost model effectively classified the region into distinct salinity zones, revealing that areas such as Ennore, Mylapore, Velachery and Egmore are highly affected by salinity, while regions like Saidapet, Anna Nagar, Kolathur and Medavakkam exhibit low to very low salinity levels.

The landuse and land cover (LULC) mapping, conducted through visual interpretation of April 2025 Landsat data following NRSC Level-3 classification, provided a detailed inventory of the study area's surface features. Urban land was the most dominant class, followed by plantations, water bodies and various scrub and agricultural categories. The results revealed that high salinity zones closely coincide with fallow land, scrubland and swampy areas highlighting the degradation of land due to salinity build up while active croplands, water body and plantations were mostly confined to low-salinity zones.

The results confirm that the combination of remote sensing indices and machine learning offers a robust framework for spatially explicit soil salinity assessment. This integrated methodology supports the findings of recent research and affirms the utility of EO data in monitoring land degradation, especially in vulnerable coastal urban environments. The insights generated from this study can inform sustainable land and water management, urban expansion planning and salinity mitigation strategies. Future work may explore temporal salinity dynamics and the integration of *in situ* soil measurements to further enhance model accuracy and decision-making.

References

1. Abdelfattah M.A., Mostafa M.H. and El-Kholy M.A., Assessment of soil salinization hazard using remote sensing and GIS in arid regions: A case study in Safaga District, Red Sea, Egypt, *Environ. Monit. Assess.*, **157**, 97–110 **(2009)**

2. Abdelaty E.F. and Aboukila E.F., Detection of soil salinity for bare and cultivated lands using Landsat ETM+ imagery data: A case study from El-Beheira Governorate, Egypt, *Alex. Sci. Exch. J.*, **38**, 644–655 **(2017)**

3. Aldakheel Y.Y., Assessing NDVI spatial pattern as related to irrigation and soil salinity management in AlHassa Oasis, Saudi Arabia, *J. Indian Soc. Remote Sens.*, **39**, 171–180 **(2011)**

4. Allbed A. and Kumar L., Soil salinity mapping and monitoring in arid and semi-arid regions using remote sensing technology: A review, *Remote Sens.*, **5**, 4384–4417 **(2013)**

5. Asfaw E., Suryabhagavan K.V. and Argaw M., Soil salinity modeling and mapping using remote sensing and GIS: The case of Wonji sugar cane irrigation farm, Ethiopia, *J. Saudi Soc. Agric. Sci.*, **15**, 196–210 **(2016)**

6. Bannari A., El-Battay A., Bannari R. and Rhinane H., Sentinel-MSI VNIR and SWIR bands sensitivity analysis for soil salinity discrimination in an arid landscape, *Remote Sens.*, **10**, 855 **(2018)**

7. Basak N., Barman A., Sundha P. and Rai A.K., Recent trends in soil salinity appraisal and management, In Soil Analysis: Recent Trends and Applications, Springer **(2020)**

8. Corwin D.L. and Yemoto K., Measurement of soil salinity: Electrical conductivity and total dissolved solids, *Soil Sci. Soc. Am. J.*, **83**, 1–2 **(2019)**

9. Deering D.W., Rouse J.W., Haas R.H. and Schell J.A., Measuring "forage production" of grazing units from Landsat MSS data, Proc. 10th Int. Symp. Remote Sens. Environ., **2**, 1169–1178 **(1975)**

10. El-Hassanin A.S., Abd El Hady A.A., Ali R.R., Abdel Maksoud K.M. and Oda M.M.M., Land resources assessment of Siwa Oasis, Western Desert, Egypt, *Plant Arch.*, **20**, 3084–3093 **(2020)**

11. Elnaggar A.A., El-Hamidi K.H., Mousa M.A. and Albakry M.F., Mapping soil salinity and evaluation of water quality in Siwa Oasis using GIS, *J. Soil Sci. Agric. Eng. Mansoura Univ.*, **8**, 9–19 **(2017)**

12. Guo B., Lu M., Fan Y., Wu H., Yang Y. and Wang C., A novel remote sensing monitoring index of salinization based on three-dimensional feature space model and its application in the Yellow River Delta of China, *Geomatics Nat. Hazards Risk*, **14**, 95–116 **(2022)**

13. Hihi S., Ben Rabah Z., Bouaziz M., Chtourou M. and Bouaziz S., Prediction of soil salinity using remote sensing tools and linear regression model, *Adv. Remote Sens.*, **8**, 77–88 **(2019)**

14. Ismail M.H., Razack M. and Elamin A.E., Assessment of groundwater recharge in arid areas using remote sensing and GIS: Wadi Watir, Sinai Peninsula, Egypt, *Hydrogeol. J.*, **21**, 853–865 **(2013)**

15. Jantaravikorn Y. and Ongsomwang S., Soil salinity prediction and its severity mapping using a suitable interpolation method on data collected by electromagnetic induction method, *Appl. Sci.*, **12**, 10550 **(2022)**

16. Karavanova A., Pachepsky Y.A. and Timlin D.J., Remote sensing of soil salinity: Potentials and constraints, *J. Appl. Remote Sens.*, **1**, 013520 **(2001)**

17. Khan S., Hanjra M.A. and Mu J., Pathways to reduce the environmental footprint of irrigation water in the Aral Sea Basin, *J. Environ. Manage.*, **75**, 133–147 **(2005)**

18. Li Z., Li Y., Xing A., Zhang J. and Liu X., Spatial prediction of soil salinity in a semi-arid oasis: Environmental sensitive variable selection and model comparison, *Chin. Geogr. Sci.*, **29**, 784–797 **(2019)**

19. Markham B.L. and Helder D.L., Forty-year calibrated record of earth-reflected radiance from Landsat: A review, *Remote Sens. Environ.*, **122**, 30–40 **(2012)**

20. Matinfar H.R., Detection of soil salinity changes and mapping land cover types based upon remotely sensed data, *Arab. J. Geosci.*, **6**, 913–919 **(2013)**

21. Moghazy N.H. and Kaluarachchi J.J., Assessment of groundwater resources in Siwa Oasis, Western Desert, Egypt, *Alex. Eng. J.*, **59**, 149–163 **(2020)**

22. Ngabire M., Wang T., Xue X., Liao J., Sahbeni G., Huang C., Duan H. and Song X., Soil salinization mapping across different sandy land-cover types in the Shiyang River Basin: A remote sensing and multiple linear regression approach, *Remote Sens. Appl. Soc. Environ.*, **23**, 100618 **(2022)**

23. Rafik A., Ibouh H., El Alaoui El Fels A., Eddahby L., Mezzane D., Bousfoul M., Mazirh A., Ouhamdouch S., Bahir M. and Gourfi A., Soil salinity detection and mapping in an environment under water stress between 1984 and 2018 (Case of the largest oasis in Africa–Morocco), *Remote Sens.*, **14**, 1606 **(2022)**

24. Salem O.H. and Jia Z., Evaluation of different soil salinity indices using remote sensing techniques in Siwa Oasis, Egypt, *Agronomy*, **14**, 759 **(2024)**

25. Song C., Woodcock C.E., Seto K.C., Lenney M.P. and Macomber S.A., Classification and change detection using Landsat TM data: When and how to correct atmospheric effects, *Remote Sens. Environ.*, **75**, 230–244 **(2001)**

26. Szatmári G., Bakacsi Z., Laborczi A., Petrik O., Pataki R., Tóth T. and Pásztor L., Elaborating Hungarian segment of the Global Map of Salt-Affected Soils (GSSmap): National contribution to an international initiative, *Remote Sens.*, **12**, 4073 **(2020)**

27. Thiam S., Villamor G.B., Faye L.C., Sène J.H., Diwediga B. and Kyei-Baffour N., Monitoring land use and soil salinity changes in coastal landscape: A case study from Senegal, *Environ. Monit. Assess.*, **193**, 259 **(2021)**

28. Wu J., Vincent B., Yang J., Bouarfa S. and Vidal A., Remote sensing monitoring of changes in soil salinity: A case study in Inner Mongolia, China, *Sensors*, **8**, 7035–7049 **(2008)**

29. Zare S., Shamsi S.R. and Abtahi S.M., Weakly-coupled geostatistical mapping of soil salinity to stepwise multiple linear regression of MODIS spectral image products, *J. Afr. Earth Sci.*, **152**, 101114 **(2019)**

30. Zhang W., Zhang W., Liu Y., Zhang J., Yang L., Wang Z., Mao Z., Qi S., Zhang C. and Yin Z., The role of soil salinization in shaping the spatio-temporal patterns of soil organic carbon stock, *Remote Sens.*, **14**, 3204 **(2022)**.

(Received 19th July 2025, accepted 18th September 2025)